Wavelet-based calculation of cerebral angiographic data from time-resolved CT perfusion acquisitions

Lukas Havla[1], Kolja M. Thierfelder[2], Sebastian E. Beyer[2], Wieland H. Sommer[2], Olaf Dietrich[1]

[1] Josef Lissner Laboratory for Biomedical Imaging, Institute for Clinical Radiology, Ludwig-Maximilians-University Hospital Munich, Germany

[2] Institute for Clinical Radiology, Ludwig-Maximilians-University Hospital Munich, Germany

Final version: *Eur Radiol.* 2015; **25**(8): 2354–2361. <URL:http://dx.doi.org/10.1007/s00330-015-3651-1>

Abstract

Objectives: To evaluate a new approach for reconstructing angiographic images by application of wavelet transforms on CT perfusion data.

Methods: 15 consecutive patients with suspected stroke were examined at a multi-detector CT acquiring 32 dynamic phases (Δt=1.5s) of 99 slices (total slab thickness 99mm) at 80kV/200mAs. 35 mL of iomeprol-350 were injected (flow rate = 4.5 mL/s). Angiographic datasets were calculated after initial rigid-body motion correction using (a) temporally filtered maximum intensity projections (tMIP) and (b) the wavelet transform (Paul wavelet, order 1) of each voxel time course. The maximum of the wavelet-power-spectrum was defined as the angiographic signal intensity. The contrast-to-noise ratio (CNR) of 18 different vessel segments was quantified and two blinded readers rated the images qualitatively using 5pt Likert scales.

Results: The CNR for the wavelet angiography (501.8±433.0) was significantly higher than for the tMIP approach (55.7±29.7, Wilcoxon test p<0.00001). Image quality was rated to be significantly higher (p<0.001) for the wavelet angiography with median scores of 4/4 (reader 1/reader 2) than the tMIP (scores of 3/3).

Conclusions: The proposed calculation approach for angiography data using temporal wavelet transforms of intracranial CT perfusion datasets provides higher vascular contrast and intrinsic removal of non-enhancing structures such as bone.

Key points

1) Angiographic images calculated with the proposed wavelet-based approach show significantly improved contrast-to-noise ratio.
2) CT perfusion based wavelet angiography is an alternative method for vessel visualization with high image quality but with limited field of view.
3) Angiographic images calculated with the proposed wavelet-based approach benefit from intrinsic removal of non-enhancing structures such as bone.

Keywords

X-ray computed tomography; Angiography; Perfusion; Wavelet analysis; Brain

Corresponding author:

Lukas Havla
Josef Lissner Laboratory for Biomedical Imaging
Institute for Clinical Radiology
Ludwig-Maximilians-University Hospital Munich
Marchioninistr. 15
81377 Munich
Germany
Fax: +49 89 7095-4627
E-mail: lukas.havla@med.uni-muenchen.de

Introduction

Information on cerebral vasculature and hemodynamics is essential in the decision making process of acute ischemic stroke. An important and commonly available imaging modality for assessing cerebral vessel occlusion is multimodal computed tomography (CT) including CT angiography (CTA) and – if available – CT perfusion imaging (CTP).

State-of-the-art CT systems provide increased scan coverage of 10 cm and more along the z-axis [1] and are particularly suited for multi-phase ("dynamic") contrast-enhanced whole-brain CT perfusion (WB-CTP) measurements. WB-CTP measurements consisting of a temporal series of whole-brain acquisitions are reliable and reproducible for assessing the volumetric perfusion deficit, for defining tissue at risk, or for diagnosing small infarctions with a cortical localization [2][3].

Multi-phase WB-CTP data can be post-processed to provide angiographic data of the scanned brain volume; e. g., the timing-invariant CTA calculation proposed by Smit et al. has been demonstrated to yield better image quality and increased overall contrast-to-noise ratio (CNR) compared to conventional CTA [4]. A particular advantage of such CTA methods from multi-phase image data is the improved visualization of leptomeningeal collaterals [5] whose blood flow possibly supplies challenged regions. Their presence is predictive of improved clinical outcome in patients with middle cerebral artery occlusion [6,7] or with intravenous thrombolysis [8]; however, those collateral vessels are not always visible in conventional CTA due to delayed contrast arrival [9,10]. Accordingly, Tan et al. conclude that a combination of CTP and CTA provide the most accurate assessment of collateral circulation [11].

In this study, we propose a new method for deriving angiographic images from dynamic volumetric data such as multi-phase WB-CTP datasets based on wavelet-transform post-processing. This new approach is evaluated qualitatively and quantitatively in WB-CTP measurements of patients without diagnostic findings and compared to the timing-invariant CTA method proposed by Smit et al. [4]

Materials and Methods

The institutional review board approved the retrospective study and waived requirement for informed consent.

Patient population

We selected 17 consecutive patients who underwent WB-CTP measurements between December 22nd, 2012 and January 31th, 2013 for suspected acute stroke but without ischemia or any other pathology on initial CT perfusion and follow-up MRI. Two patients had to be excluded: one because of strong motion artifacts, which could not be corrected by image co-registration, and one because of missing reconstructions in 1.5 mm slice thickness. Hence, we examined cerebral CT perfusion data of 15 patients (7 female, mean age 71, range 17–97).

CT examination protocol

All patients were examined at a multi-detector 2 × 128 CT system (SOMATOM Definition Flash, Siemens Healthcare, Forchheim, Germany) in single-source mode. The continuous acquisition of 32 dynamic phases took 48 s (mean temporal resolution: 1.5 s) using an adaptive spiral scanning technique. 99 axial slices with slice thickness of 1.5 mm and increment of 1.0 mm were reconstructed (kernel: H20f). Tube voltage and current were set to 80 kV and 200 mAs, respectively. 35 mL of iomeprol-350 (Imeron 350, Bracco Imaging Deutschland, Konstanz, Germany) were injected at a flow rate of 4.5 mL/s, followed by a saline flush of 40 mL at the same rate.

Image post-processing

32 × 99 (phases × slices) CT DICOM images from each patient were imported into in-house developed software (PMI, Platform for Medical Imaging v0.4 [12]) based on IDL 8.3 (Exelis Visual Information Solutions Inc., Boulder, CO, USA). On each 4D CT volume, rigid-body motion correction was performed with the elastix toolbox [13] using a binary mask that contained all voxels with density > 0 HU at the first phase. After motion correction, angiography data was calculated using the timing-invariant CTA method proposed by Smit et al. [4] and the proposed wavelet-based approach as described below.

Timing-invariant CTA

To obtain 3D CT angiography data, the temporal maximum intensity projection (tMIP) [14] of the multi-phase CT data, i. e., the maximal signal of each voxel time series, was calculated, which preferentially displays contrast-enhanced structures such as vessels. To improve image quality without compromising the spatial resolution, temporal filtering was applied prior to the creation of tMIP-CT angiographic images using a Gaussian filter with the optimal width (standard deviation) of 1.5 s (found by Smit et al. [4]).

Wavelet-based CTA (WBA)

The wavelet transform was originally introduced by Morlet [15] and Grossmann [16] in the 1980s, and is nowadays frequently used in signal [17] and image processing applications, e g. for noise reduction or data compression. In the present study, the wavelet transform is applied in the temporal domain on the one-dimensional signal time courses of each voxel as an alternative to the tMIP calculation to derive 3D angiographic images.

The wavelet transform is based on a complex-valued function, $\Psi_0(\eta)$, – the *mother wavelet* – dependent on a (dimensionless) time parameter η [18]. Since wavelets are normally concentrated on some finite domain they allow signal analysis by translation (parameter *t*) and scaling (parameter *s*) of the mother wavelet according to:

$$\Psi_{s,t}(\eta) = |s|^{(-1/2)}\,\Psi_0\left(\frac{\eta - t}{s}\right).$$

The continuous wavelet transform $\tilde{f}(s,t)$ of $f(\eta)$ is defined as the convolution:

$$\tilde{f}(s,t) = \int f(\eta)\,\overline{\Psi}_{s,t}(\eta)\,\mathrm{d}\,\eta$$

with $\overline{\Psi}_{s,t}$:= complex conjugate of $\Psi_{s,t}$

For discrete data $f_n = f(n\cdot\delta t)$ with $n = 0\ldots T-1$ and spacing δt in the temporal domain, the wavelet transform is a matrix $\tilde{f}_{s,t}$ with indices *s* and *t* [19]:

$$\tilde{f}_{s,t} = \sum_{n=0}^{T-1} f_n \cdot \overline{\Psi}_{s,t\cdot\delta t}(n\cdot\delta t)\,.$$

For our study, we used the Paul wavelet of order *m = 1* (Figure 1) defined as [19]:

$$\Psi_0(\eta) = \frac{2^m\, i^m\, m!}{\sqrt{\pi(2m)!}}\,(1 - i\eta)^{-(m+1)}.$$

The wavelet transform was calculated for *T = 32* equidistant time points (*t* = 0, 1, … 31) and for *S = 128* scaling factors (*s* distributed logarithmically [19] between 4.5 and 18). For each time series $f_n(x,y,z)$ at voxel position (*x,y,z*), the wavelet transform $\tilde{f}_{s,t}(x,y,z)$ is a 2D matrix of size *S* × *T*, whose squared norm yields the *wavelet power spectrum*. The maximal value of the power spectrum was then interpreted as angiographic signal intensity (Figure 2):

$$\text{angiography}\quad A(x,y,z) = \max_{s,t}\left(\left|\tilde{f}_{s,t}(x,y,z)\right|^2\right).$$

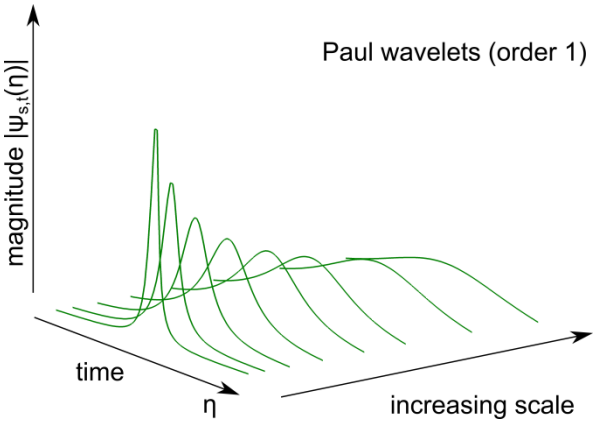

Figure 1. The magnitude of the complex Paul wavelet function $\Psi_{s,t}(\eta)$ (of order 1) at different scales s is shown. In this study, the Paul wavelet was chosen because its magnitude curve nicely resembles bolus flow in vasculature.

Quantitative evaluation

Contrast-to-noise ratio (CNR) was defined as the intensity difference between the foreground structure of interest and an adjacent background region divided by the standard deviation of the background signal [4]. For 18 vessel segments (2× internal carotid / 1× basilar / 2× M1 middle cerebral / 2× P1 posterior cerebral / 2× M2 middle cerebral arteries, 2× leptomeningeal collaterals, 1× sagittal / 2× transverse / 2× sigmoid sinuses, 2× bridging veins to the sagittal sinus), CNR was calculated by selecting foreground circular regions of interest (ROIs) with varying size (29.9±30.0 voxels) adapted to the vessel anatomy. For each segment, an individual background ROI (circular, 314 voxels) was manually placed adjacent to the vessel in non-enhanced tissue to minimize the influence of vary-

ing noise behavior throughout the 3D volume and streaking artifacts [20].

Identical ROIs were selected for both assessed post-processing methods (timing-invariant tMIP-CTA and wavelet-based CTA). To directly compare the CNR of both assessed post-processing methods, the CNR ratio $CNR_{wavelet}/CNR_{tMIP}$ was calculated for all ROIs. A CNR ratio >1 indicates higher CNR for WBA.

Comparison of CTA methods qualitatively

Nine different aspects of subjective image quality were rated using 5-point Likert scales (cf. **Table 3**) by two blinded and experienced readers (W.H.S. and K.M.T., both with over 6 years of experience in neuroimaging). The subcategories were vascular noise, vascular contour/vessel sharpness, detail visibility of medium arteries, small arteries, leptomeningeal collaterals, and bridging veins, the overall image quality, venous superimposition and motion artifacts.

Statistical analysis

We performed all statistical analysis using R (v3.0.1; R Foundation for Statistical Computing, Vienna, Austria). Differences in CNRs were tested with a paired Wilcoxon signed rank test, and the agreement between qualitative evaluations of both readers was measured with Cohen's κ. Differences with p-values <0.05 were considered as statistically significant.

Results

Quantitative analysis

The mean CNR (averaged over all patients and vessel segments) for the wavelet angiography (501.8±433.0) was nine times higher than for the timing-invariant tMIP approach (55.7±29.7, Wilcoxon test p<0.00001). **Table 1** shows the calculated ratios CNR_{wave}/CNR_{tMIP} for all analyzed vessel segments and

Table 2 lists the intensity difference and noise values separately. Among the different vessel segments, ratios ranging from 1.6 to 67.2 (mean 8.8±6.5) were achieved, meaning that throughout the study a better CNR of the proposed method was found (Figure 3).

Qualitative evaluation

The new method was rated significantly higher (p<0.01) in following qualitative categories: *vascular noise* (WBA: 4/4 (reader 1/reader 2) vs. tMIP: 3/3), *vascular contour* (4/4 vs. 3/3), *details small* (4/4 vs. 2/2), *leptomeningeal collaterals* (4/4 vs. 2/2), *bridging veins* (4/4 vs. 2/2), and *overall image quality* (4/4 vs. 3/3). There was no significant difference with respect to the criteria *details middle* (4/4 vs. 4/4), *venous superimposition* (3/3 vs. 3/3), and *motion artifacts* (3/3 vs. 3/3). To summarize, in six of nine categories WBA scored significantly higher than tMIP. **Table 3** contains the detailed results.

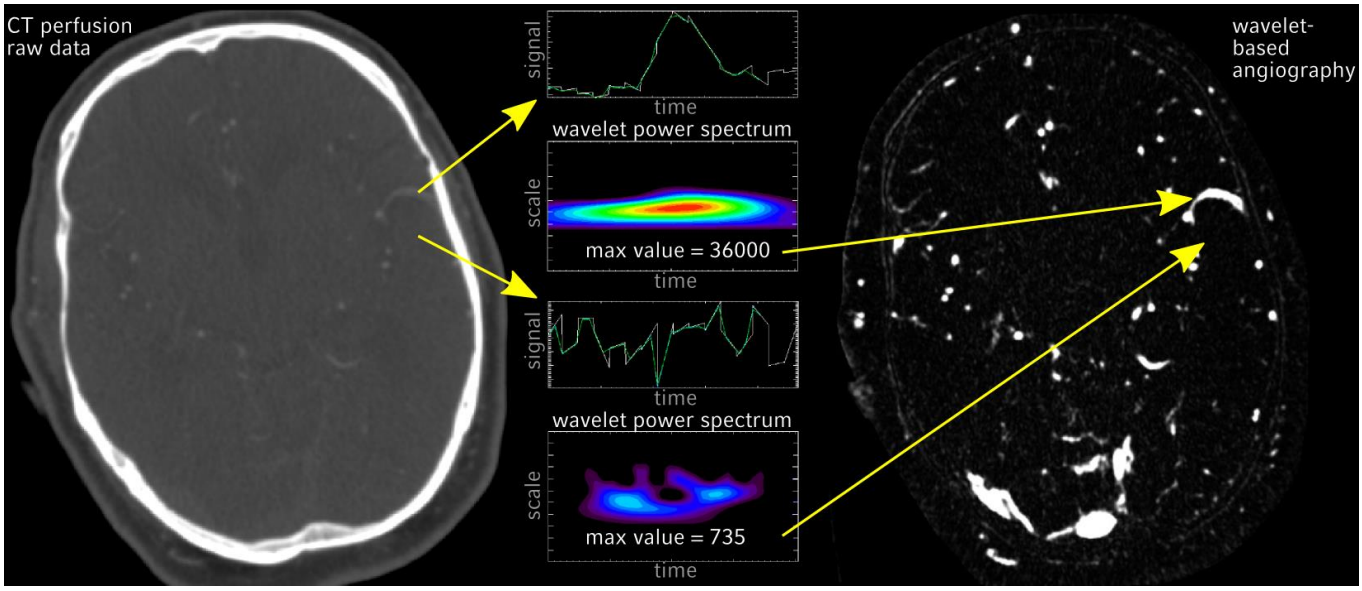

Figure 2. Calculation of angiographic images by voxel-by-voxel application of the wavelet transform on CT perfusion data. The wavelet power spectrum displays the total amount of convolution between the wavelet at scale s and at time t with the voxel time series $f_n(x,y,z)$. The right panel shows the maximal values from each WPS.

Table 1: Quantitative analysis of the wavelet method compared to the filtered tMIP approach: relative contrast-to-noise ratios.

Quantitative results				
			ratio CNR_{WBA}/CNR_{tMIP}	
			Mean ± S.D. (N=15)	**(Min-Max)**
Caudal	**A. carotis int.**	Left	9.0±4.6	(4.6-21.9)
		Right	9.7±4.5	(4.7-22.3)
	A. basilaris		8.8±3.8	(2.8-15.4)
Circulus	**M1**	Left	9.3±3.9	(3.8-21.5)
		Right	8.5±3.1	(4.5-18.7)
	A. cerebri post.	Left	8.9±8.1	(3.3-37.6)
		Right	6.3±3.0	(2.7-12.6)
Periphery	**M2**	Left	8.0±3.9	(3.0-17.0)
		Right	8.1±3.7	(4.6-18.8)
	lepto. collaterals	Left	7.1±4.3	(1.6-15.1)
		Right	7.0±3.4	(1.9-13.7)
Venous	**Superior sagittal sinus**		13.1±5.1	(5.5-23.0)
	Transverse sinus	Left	7.0±3.3	(2.3-14.9)
		Right	9.7±8.2	(2.5-31.6)
	Sigmoid sinus	Left	11.3±11.3	(2.1-50.0)
		Right	8.4±2.8	(3.6-12.6)
	Bridging veins	Left	7.4±3.1	(2.8-13.2)
		Right	10.9±15.4	(2.7-67.2)
		Total	8.8±6.5	(1.6-67.2)

Table 2: Overview of contrast (defined as signal difference between vessel and background) and noise values for the evaluated vessel segments.

Details of the quantitative evaluation						
			Contrast (signal difference)		**Noise**	
			WBA	**tMIP**	**WBA**	**tMIP**
Caudal	**A. car. int.**	Left	236,162.8±141,681.4	461.6±118.8	334.8± 95.8	5.9± 1.4
		Right	251,273.5±125,955.6	469.7±118.6	363.2±146.8	6.6± 2.3
	A. basil.		209,750.1±130,121.7	415.2±119.4	368.5±110.5	6.5± 1.5
Circulus	**M1**	Left	205,237.6±130,390.4	421.0±114.7	286.2± 72.4	5.7± 1.3
		Right	194,971.5±103,022.5	411.0± 96.1	292.9± 77.3	5.4± 1.1
	A. cer. p.	Left	110,721.9±68,055.7	300.2± 86.6	291.6± 51.6	6.8± 2.8
		Right	118,620.1±76,740.1	307.5± 88.7	299.5±107.1	5.0± 0.9
Periphery	**M2**	Left	97,876.0±45,694.8	286.5± 71.9	239.9± 50.8	5.7± 2.0
		Right	99,842.4±46,318.4	294.6± 69.5	243.9± 46.3	5.8± 1.2
	lepto. coll.	Left	52,940.4±35,114.3	254.8± 67.6	266.9±148.6	8.2± 3.3
		Right	51,500.5±39,528.7	218.2± 86.4	248.0± 77.5	8.4± 3.2
Venous	**Sup. sag. S**		250,519.4±144,315.2	475.8±112.8	286.5±110.0	7.2± 2.4
	Trans. S	Left	165,327.9±110,001.5	391.5±118.2	319.1± 79.7	5.7± 1.1
		Right	185,054.2±115,532.4	421.0±110.7	305.0±103.5	6.2± 1.3
	Sigmoid S	Left	194,378.0±143,590.1	427.6±129.5	496.0± 99.9	11.3± 3.9
		Right	212,953.2±143,540.4	403.3±118.5	527.4±142.5	9.2± 2.1
	Bridg. veins	Left	27,711.0±29,731.9	158.1±100.2	213.8± 70.1	9.6± 2.4
		Right	20,121.7±9,936.5	176.7±136.7	203.5± 42.4	10.4± 3.1
All values are given as mean ± standard deviation						

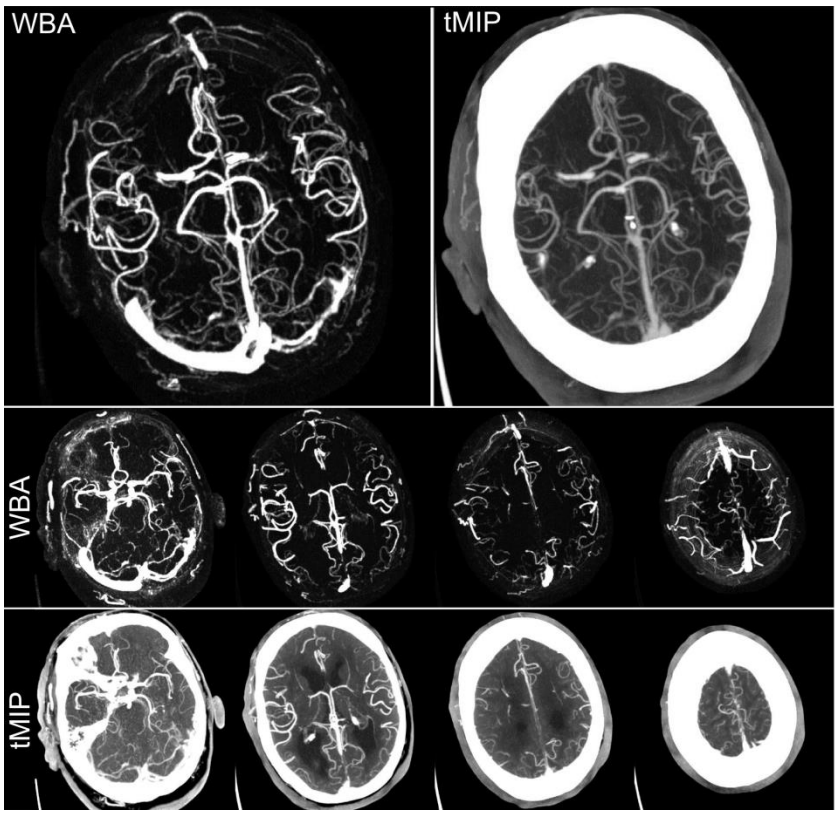

Figure 3. Exemplary angiographic images of one patient (male, 76y) are displayed. In the top row, an 60 mm maximum-intensity-projection (MIP) along z-axis is compared. The second row shows 20 mm MIPs at different slice positions of the same patient.

Table 3: Qualitative analysis (5pt Likert scale) of WBA and tMIP images by two blinded readers.

Results of qualitative Evaluation							
		Median score					
	Reader	**WBA**	**tMIP**	**WBA better [%]**	**Equal [%]**	**tMIP better [%]**	**p-value**
Vascular noise	**#1**	4	3	60.0	40.0	0.0	0.003†
0: non diagnostic 4: optimal	**#2**	4	3	66.7	33.3	0.0	0.004†
	Kappa	*0.583*	*0.571*				
Vascular contour	**#1**	4	3	66.7	33.3	0.0	0.002†
0: non diagnostic 4: optimal	**#2**	4	3	66.7	33.3	0.0	0.003†
	Kappa	*1.000*	*0.198*				
Details middle	**#1**	4	4	20.0	80.0	0.0	0.149
0: non diagnostic 4: optimal	**#2**	4	4	13.3	86.7	0.0	0.346
	Kappa	*1.000*	*0.826*				
Details small	**#1**	4	2	100.0	0.0	0.0	0.0004†
0: non diagnostic 4: optimal	**#2**	4	2	93.3	6.7	0.0	0.001†
	Kappa	*0.853*	*0.615*				
Leptomeningeal collaterals	**#1**	4	2	100.0	0.0	0.0	0.0005†
	#2	4	2	100.0	0.0	0.0	0.0004†
0: non diagnostic 4: optimal	**Kappa**	*0.643*	*0.500*				
Bridging veins	**#1**	4	2	93.3	6.7	0.0	0.001†
0: non diagnostic 4: optimal	**#2**	4	2	93.3	6.7	0.0	0.001†
	Kappa	*0.750*	*0.455*				
Overall image quality	**#1**	4	3	80.0	20.0	0.0	0.001†
0: non diagnostic 4: optimal	**#2**	4	3	93.3	6.7	0.0	0.0002†
	Kappa	*1.000*	*0.674*				
Venous Superimposition	**#1**	3	3	13.3	80.0	6.7	0.773
	#2	3	3	0.0	100.0	0.0	1.000
0: none 4: strong	**Kappa**	*0.559*	*0.524*				
Motion artifacts	**#1**	3	3	0.0	93.3	6.7	1.000
0: none 4: strong	**#2**	3	3	0.0	93.3	6.7	1.000
	Kappa	*0.783*	*0.773*				

†: significant

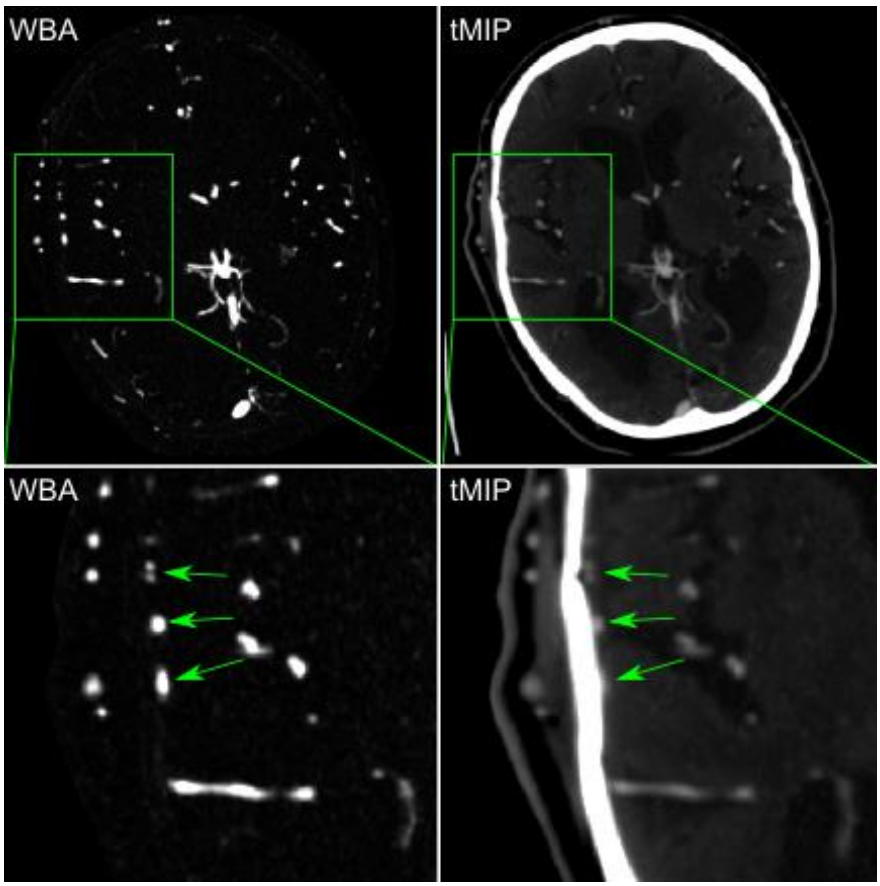

Figure 4. Visibility of vessels close to bone is improved. Arrows point to small vessels close to the calvaria.

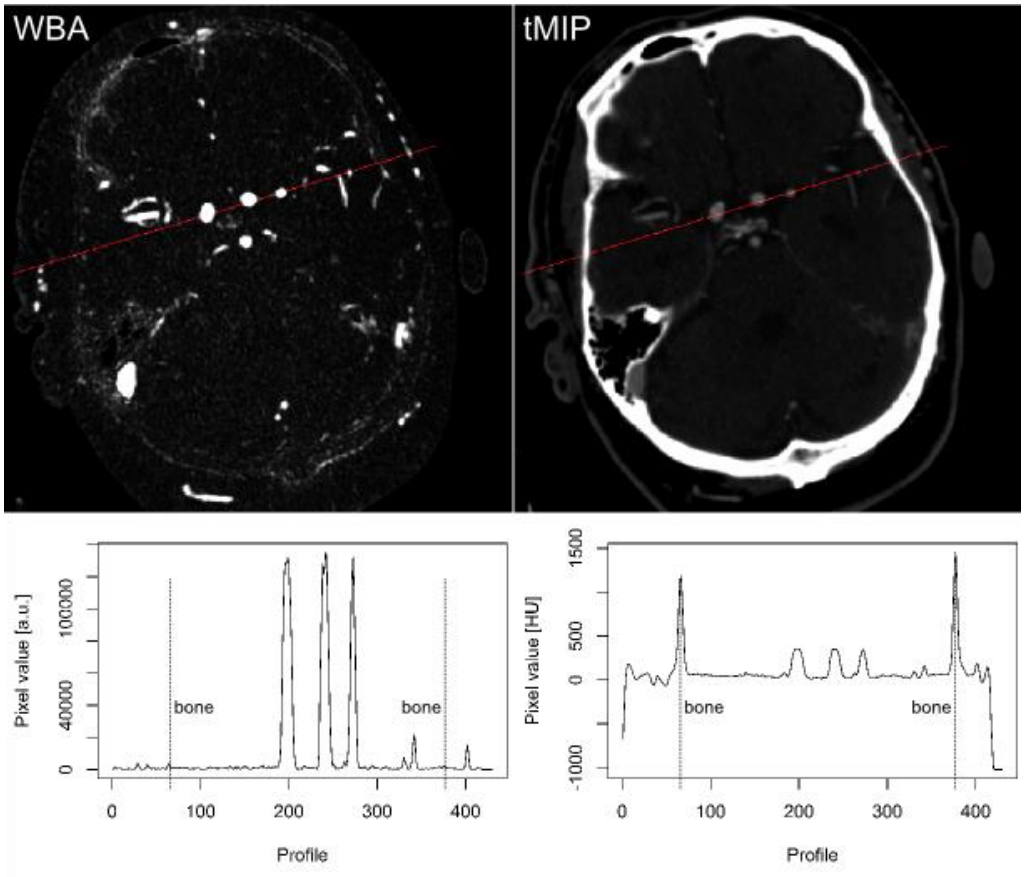

Figure 5. Profile view of one slice. Red line (exactly identical on both sides) shows the voxels used for the profile plots in the second row. The WBA data (left column) lacks bone signal as opposed to the tMIP profile.

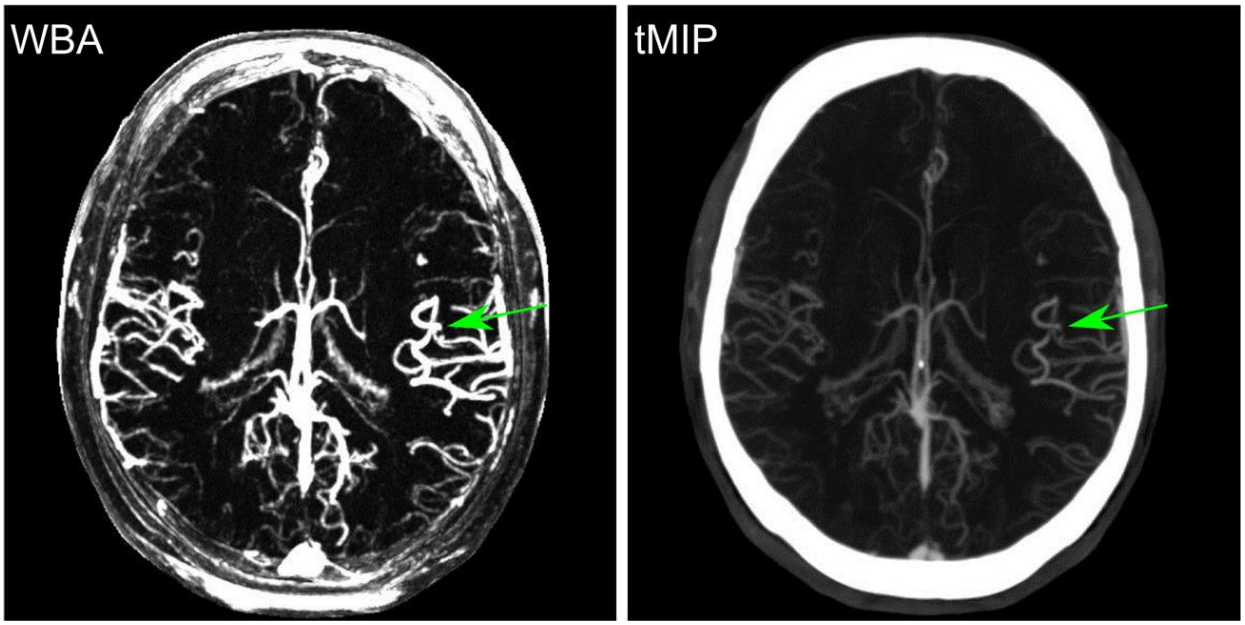

Figure 6. Exemplary patient data of a 59 y/o male patient with pathology (wavelet-based angiography on the left ,tMIP angriography on the right). Images are presented as maximum-intensity projections along the z-axis over 10 axial slices. The green arrow points to the occlusion of a M3 branch of the left middle cerebral artery.

Inter-observer Cohen's κ for all 270 observations was κ=0.754 indicating "substantial" agreement [21]; additionally, κ was calculated for each subcategory (N=9) and separately listed for both angiographic method ranging from κ=0.198 ("slight") to κ=1 ("almost perfect" agreement).

The improved visibility of small vessel details is illustrated in Figure 4 and Figure 5. Figure 4 shows that vessels close to the calvaria are better visible since bony and stationary structures are excluded from the angiographic image. Figure 5 displays a voxel-by-voxel comparison between exemplary images from both methods. The new method almost perfectly suppresses signal from non-enhancing tissue such as bone.

In Figure 6 one exemplary case of a patient with pathological finding (vessel occlusion) is presented to demonstrate the potential of our new approach.

Discussion

In this study, we evaluated a new wavelet-based method to calculate high-quality angiographic images from whole-brain CT perfusion data. The approach replaces the previously proposed voxelwise calculation of the filtered tMIP by the voxelwise calculation of the wavelet power spectrum, the maximum of which is then used as angiographic image intensity. Using wavelet transforms, a nine-fold, statistically significant increase of CNR can be achieved compared to tMIP methods. The higher CNR and increase in image quality (plus method-inherent bone subtraction) can be expected to be especially important for the assessment of small peripheral branches and leptomeningeal collaterals, which are not always visible in conventional CTA [9, 10] but whose presence can be predictive of improved clinical outcome [6, 7].

Generally, approaches that calculate angiographic data from CT perfusion data such as tMIP techniques offer improved image quality over conventional and dynamic CTA [4]. There are, however, still many cases in which both CTP and follow-up MRI show infarction but the corresponding occlusion cannot be demonstrated using CTA or tMIP images. Thus, it may be assumed that the increase of CNR (resulting from the proposed wavelet approach) will improve the detection rate in small vessel occlusions.

As the technique proved to be very robust (only one patient had to be excluded due to motion artifacts), one may consider to replace conventional CTA by CTP-based angiographic techniques in certain cases. As an advantage, the radiation dose would be reduced due to the omitted dedicated CT angiography sequence. However, since CTA covers all vessels from the aortic arch to the vertex, it appears not recommendable to waive CTA as long as carot-

id or vertebral arteries might play a role in the treatment of the patient.

The proposed approach is currently based on the ad-hoc choice of a Paul wavelet of order $m = 1$ as mother wavelet. Future studies are required to quantify the influence of the chosen mother wavelet on the image quality of the calculated angiography datasets.

Calculation of the timing-invariant tMIP CTA took 14–15 minutes on a 64-bit personal computer equipped with 16 GB RAM and a standard Intel i5 processor. The computation time of the wavelet maps is strongly dependent on the initial transform parameters such as number of scale steps. In this initial assessment, the wavelet transform was evaluated for a large number of 128 scale steps ranging from 4.5 to 18,. The resulting calculation time of 480 minutes is prohibitive for clinical application in the moment but it is rather a coding issue than a substantial problem of our method; by reducing the number and range of scale steps as well as applying multi-core parallel processing and optimized wavelet-transform code, it can easily be reduced (without even changing the hardware) by a factor of 100 to about 5 minutes.

A potential limitation of the proposed method is the loss of the Hounsfield unit scale during (non-linear) post-processing; however, conventional CT perfusion and angiographic images are still available. A second limitation of our study is that we did not compare our method to the standard CTA data, since it was previously demonstrated that timing-invariant tMIP methods provide superior image quality [4]. As a further limitation, we included only patients without findings to rule out pathology-based variations in CNR; future studies need to investigate the applicability of our new method in patients with positive vascular findings;, image data from one patient with pathology were presented in Fig. 6. As final limitation, we would like to mention the requirement of a current high-performance CT system capable of rapid dynamic CTP imaging with sufficient axial coverage.

In summary, the proposed wavelet-based angiography method provides nine-fold and statistically significant increase in CNR compared to previously suggested techniques as well as intrinsic removal of non-enhancing structures such as bone.

References

1. Morhard D, Wirth CD, Fesl G, et al. (2010) Advantages of extended brain perfusion computed tomography: 9.6 cm coverage with time resolved computed tomography-angiography in comparison to standard stroke-computed tomography. Invest Radiol 45:363–9

2. Thierfelder KM, Sommer WH, Baumann AB, et al. (2013) Whole-brain CT perfusion: reliability and reproducibility of volumetric perfusion deficit assessment in patients with acute ischemic stroke. Neuroradiology 55:827–35

3. Thierfelder KM, von Baumgarten L, Löchelt AC, et al. (2014) Diagnostic accuracy of whole-brain computed tomographic perfusion imaging in small-volume infarctions. Invest Radiol 49:236–42

4. Smit EJ, Vonken E, van der Schaaf IC, et al. (2012) Timing-invariant reconstruction for deriving high-quality CT angiographic data from cerebral CT perfusion data. Radiology 263:216–25

5. Smit EJ, Vonken E, van Seeters T, et al. (2013) Timing-invariant imaging of collateral vessels in acute ischemic stroke. Stroke 44:2194–9

6. Liebeskind DS (2003) Collateral circulation. Stroke 34:2279–84

7. McVerry F, Liebeskind DS, Muir KW (2012) Systematic review of methods for assessing leptomeningeal collateral flow. AJNR Am J Neuroradiol 33:576–82

8. Saarinen JT, Rusanen H, Sillanpää N (2014) Collateral Score Complements Clot Location in Predicting the Outcome of Intravenous Thrombolysis. AJNR Am J Neuroradiol 35:1892-6

9. Bae KT (2010) Intravenous contrast medium administration and scan timing at CT: considerations and approaches. Radiology 256:32–61

10. Calleja a I, Cortijo E, García-Bermejo P, et al. (2013) Collateral circulation on perfusion-computed tomography-source images predicts the response to stroke intravenous thrombolysis. Eur J Neurol 20:795–802

11. Tan JC, Dillon WP, Liu S, et al. (2007) Systematic comparison of perfusion-CT and CT-angiography in acute stroke patients. Ann Neurol 61:533–43

12. Sourbron S, Biffar AF, Ingrisch M, et al. (2009) PMI0.4: platform for research in medical imaging. Proc. ESMRMB, Antalya

13. Klein S, Staring M, Murphy K, et al. (2010) elastix: a toolbox for intensity-based medical image registration. IEEE Trans Med Imaging 29:196–205

14. Beier J, Büge T, Stroszczynski C, et al. (1998) [2D and 3D parameter images for the analysis of contrast medium distribution in dynamic CT and MRI]. Radiologe 38:832–40

15. Morlet J, Arens G, Fourgeau E, Glard D (1982) Wave propagation and sampling theory—Part I: Complex signal and scattering in multilayered media. GEOPHYSICS 47:203–221

16. Grossmann A, Morlet J (1984) Decomposition of Hardy Functions into Square Integrable Wavelets of Constant Shape. SIAM J Math Anal 15:723–736

17. Daubechies I (1990) The wavelet transform, time-frequency localization and signal analysis. IEEE Trans Inf Theory 36:961–1005

18. Farge M (1992) Wavelet Transforms And Their Applications To Turbulence. Annu Rev Fluid Mech 24:395–457

19. Torrence C, Compo GP (1998) A Practical Guide to Wavelet Analysis. Bull Am Meteorol Soc 79:61–78

20. Boas FE, Fleischmann D (2012) CT artifacts: causes and reduction techniques. Imaging Med 4:229–240

21. Landis JR, Koch GG (1977) The measurement of observer agreement for categorical data. Biometrics 33:159–74